AIP | Physics of Plasmas

Controlling the betatron oscillations of a wakefield-accelerated electron beam by temporally asymmetric laser pulses

Inhyuk Nam, Min Sup Hur, Han Sup Uhm, Nasr A. M. Hafz, and Hyyong Suk

Citation: Phys. Plasmas **18**, 043107 (2011); doi: 10.1063/1.3577566
View online: http://dx.doi.org/10.1063/1.3577566
View Table of Contents: http://pop.aip.org/resource/1/PHPAEN/v18/i4
Published by the AIP Publishing LLC.

Controlling the betatron oscillations of a wakefield-accelerated electron beam by temporally asymmetric laser pulses

Inhyuk Nam,[1] Min Sup Hur,[2] Han Sup Uhm,[3,4] Nasr A. M. Hafz, and [4,a)] Hyyong Suk,[4,b)]
[1]*Graduate Program of Photonics and Applied Physics, Gwangju Institute of Science and Technology (GIST), Gwangju 500-712, Korea*
[2]*School of Electrical and Computer Engineering, Ulsan National Institute of Science and Technology (UNIST), Ulsan 689-798, Korea*
[3]*Electrophysics Department, Kwangwoon University, Seoul 139-701, Korea*
[4]*Advanced Photonics Research Institute, Gwangju Institute of Science and Technology (GIST), Gwangju 500-712, Korea*

(Received 11 January 2011; accepted 16 March 2011; published online 28 April 2011)

Based on two-dimensional particle-in-cell simulations, we investigated the electron beam's transverse oscillations by temporally asymmetric laser pulses in laser wakefield acceleration. Of particular interest in this article are the effects of ultrashort laser pulses having sharp rising and slow falling time scales. In this situation, the accelerated electron beam interacts directly with the laser field and undergoes transverse oscillations due to a phase-slip with the laser field. This oscillation can be matched with the betatron oscillation due to the focusing force of the ions, which can lead to a large transverse oscillation amplitude due to the resonance between them. Furthermore, in this case, the electron beam can be microbunched at the laser wavelength, which may provide the possibility for generation of a coherent synchrotron radiation. © *2011 American Institute of Physics*. [doi:10.1063/1.3577566]

I. INTRODUCTION

Laser wakefield acceleration (LWFA) scheme utilizes large-amplitude plasma waves for accelerating electrons to relativistic energies over an extremely short distance. Therefore, this scheme is promising as a new technology that could lead to downsizing future high-energy accelerators.[1] One of the recent breakthroughs in the LWFA is the generation of quasimonoenergetic electron beams with energies of a few hundred MeV ~GeV.[2–6] When an intense laser pulse propagates in plasma, an ion cavity is formed and some electrons are self-injected into the acceleration phase of the ion bubble. As the laser propagates further in the plasma, the bubble size and shape evolve. As a result of this evolution, multiple monoenergetic electron injections were observed.[7,8] As the electron bunch is accelerated along the bubble, it experiences a transverse force, which leads to betatron oscillations, emitting synchrotron radiation in the forward direction.[9–11] Hence, a laser wakefield accelerator itself can serve as an extremely compact synchrotron light source.

During acceleration in the ion cavity, electrons undergo the betatron oscillation with a wavelength λ_β due to the focusing force by ions, and the electrons can emit the synchrotron radiation. The spectrum of this radiation is characterized by the wiggler strength parameter $a_\beta = 2\pi\gamma r_\beta/\lambda_\beta$, where r_β is the amplitude of the betatron oscillation and γ is the relativistic energy factor. For $a_\beta \ll 1$, the radiation is monochromatic, while for $a_\beta \gg 1$, the spectrum of betatron radiation is the synchrotronlike spectrum characterized by the critical frequency $\omega_c = 3/4\gamma^3\, c\, r_\beta\, k_\beta$, where c is the speed of light in free space and k_β is the wavenumber of the betatron oscillation. Hence, higher photon energies can be obtained by increasing γ and r_β for a fixed electron density n_e.

In the bubble regime, when the laser pulse duration is comparable to one-half of the plasma period, a strong plasma wakefield can be effectively excited. It is also found that an asymmetric laser pulse with a sharp rise time and a slow fall time can produce significantly larger wake waves than the case of the symmetric pulse. Thus, asymmetric laser pulses are more effective in electron trapping and in the enhancement of the maximum electron beam energy.[12,13] When the pulse duration is longer than half the plasma period, the accelerated electron beam can interact with the laser field. Due to the interaction, an elliptic spatial electron beam profile was observed with an increased emittance along the laser polarization direction and this led to an elliptic distribution of x-ray radiation.[9,14–16] In Ref. 17, in the two-laser pulse colliding method, an increased beam emittance along the laser polarization was explained as the result of the betatron oscillation due to the laser field of the injection pulse. In this method, two well-synchronized counter propagating pulses are required in order that the electrons interact with the laser field.[18]

However, the transverse motion of the accelerated electrons due to a single asymmetric laser pulse having a sharp rise time and a slow fall time scale has not been well investigated so far. In this paper, therefore, we investigate the effects of a long asymmetric laser pulse in electron beam's transverse oscillation. In the case of a long asymmetric laser pulse, the sharply rising part can effectively excite a stronger wake wave with self-injection, and then the accelerated electrons interact with the slow falling part of the laser pulse,

a)Electronic mail: nasr@gist.ac.kr. Present address: Shanghai Jiao Tong University, Physics Department, Shanghai 200240, China.
b)Electronic mail: hysuk@gist.ac.kr.

leading to significant increase in amplitude of the transverse oscillation of the accelerated electrons. Hence, the amplitude of the transverse oscillations of the electrons can increase to the ion cavity size approximately. Therefore, this large-amplitude can lead to the generation of higher synchrotron photon energies. Furthermore, in this case, the electron beam can be microbunched at the laser wavelength, which may lead to the generation of a coherent radiation. With a simple harmonic oscillator model, we described the dynamics of the electrons due to the laser field and the focusing field of ions. The electrons oscillate due to the difference in the phase velocity of the laser field and the electrons. The transverse amplitude oscillations increased due to a resonance between the focusing field of ion cavity and the laser fields. Some details about such phenomena are presented in this paper.

II. SIMULATIONS WITH ASYMMETRIC PULSES

For our studies, we used the fully relativistic 2D particle-in-cell (PIC) code named UG-PIC, which was recently developed at UNIST. The code incorporates a standard Yee-mesh scheme for the electromagnetic field solver and Villasenor-Buneman method for electric current from the simulation particles. The code employs a moving window that moves along the x-axis at the speed of light. The two-dimensional simulation box size is $100\,\mu\text{m} \times 80\,\mu\text{m}$ in longitudinal and transverse directions. The grid resolution is chosen to be $\Delta x = \lambda_0/20$, $\Delta y = \lambda_0/4$, where λ_0 is the wavelength of the laser, and five particles per cell are used. In the simulations, we used both symmetric and asymmetric laser pulses for comparison studies, where the laser pulses are linearly polarized in both cases.

The symmetric laser pulse with a Gaussian shape has a pulse duration (FWHM) of 35 fs and the asymmetric pulse has several different ratios of rising and falling times. In both cases, the laser beam has a normalized vector potential of $a_0 = 2$, a spot size (FWHM) of $w_0 = 12.5\,\mu\text{m}$ and a wavelength of $\lambda_0 = 0.8\,\mu\text{m}$. Here, the normalized vector potential is defined by $a_0 = eE/mc\omega$, where E is the laser electric field, ω is the laser frequency, and e and m are the electron charge and mass, respectively. The laser propagates through an underdense plasma slab along the x-direction, and the plasma density profile used in the current study is shown in Fig. 1. An initial plasma density hike of $1 \times 10^{19}\,\text{cm}^{-3}$ is artificially assumed in the simulations to allow for early electron injection into the first plasma wave period.[19] After this hike, the laser propagates into 2.3 mm-long uniform plasma with a lower density of $n_2 = 5 \times 10^{18}\,\text{cm}^{-3}$, in Fig. 1. The ramps from 0 to n_1 is $100\,\mu\text{m}$ and from n_1 to n_2 is $30\,\mu\text{m}$, where both scale lengths are longer than λ_p. This density hike could be generated by plasma expansion as a result of a counter-crossing laser beam.[20]

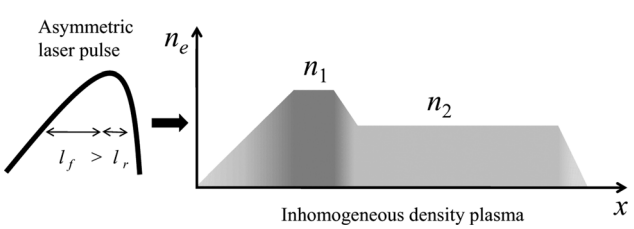

FIG. 1. Schematic of the density profile of a plasma slab and an asymmetric laser pulse. The density of the first plateau is $n_1 = 1 \times 10^{19}\,\text{cm}^{-3}$ with a length of $100\,\mu\text{m}$, and the second plateau is $n_2 = 5 \times 10^{18}\,\text{cm}^{-3}$ with a length of 2.3 mm. The ramp scale lengths from 0 to n_1 and from n_1 to n_2 are $100\,\mu\text{m}$ and $30\,\mu\text{m}$, respectively.

III. RESULTS AND DISCUSSIONS

For comparison studies, a symmetric laser pulse with a duration of 35 fs and an asymmetric pulse with rising and falling times of 7 and 28 fs, respectively, were used. In addition, we also used a longer asymmetric pulse having a pulse duration of 47.5 fs with rising and falling times of 17.5 and 30 fs, respectively. Figures 2(a) and 2(c) show the plasma density distribution of the first ion cavity for 35 fs symmetric pulse at $t = 1.8$ and 7.3 ps. Electron trapping and injection into the first ion cavity took place in the downward density gradient region. Then, the laser pulse propagates into the lower density n_2 plateau, where the cavity size is large, $\lambda_p \approx 15\,\mu m$. As the electron beam reaches the cavity center, it experiences a betatron oscillation with $1\,\mu\text{m}$ amplitude and an increase in its transverse emittance. The asymmetric laser pulse (rising time of 7 fs and falling time of 28 fs) results are shown in Figs. 2(b) at $t = 1.53$ ps and 2(d) at $t = 7.1$ ps. In this case, the accelerated electrons are under the strong influence of the transverse electric field of the laser tail. The simulation result shows that the amplitude of the betatron oscillation increases by a of factor 2, compared with the case of the symmetric laser pulse. Additionally, the electron beam is longitudinally microbunched at the laser wavelength which, in turn, leads to a resonance with the laser field, resulting in enhanced amplitude of the transverse oscillation. However, the energy of electrons of the asymmetric pulse is

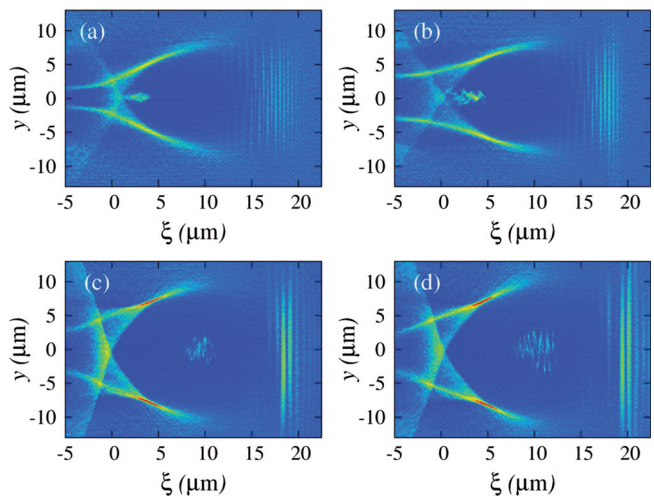

FIG. 2. (Color online) Electron density distributions in the first ion cavity for the case of a symmetric laser pulse with a duration of 35 fs (a) at 1.8 ps and (c) at 7.3 ps. Shown in (b) and (d) are the electron density distributions at 1.53 ps and at 7.1 ps, respectively, for the case of an asymmetric laser pulse which has a falling duration of 28 fs and a rising duration of 7 fs. ξ denotes the distance from the starting point of the bubble along x.

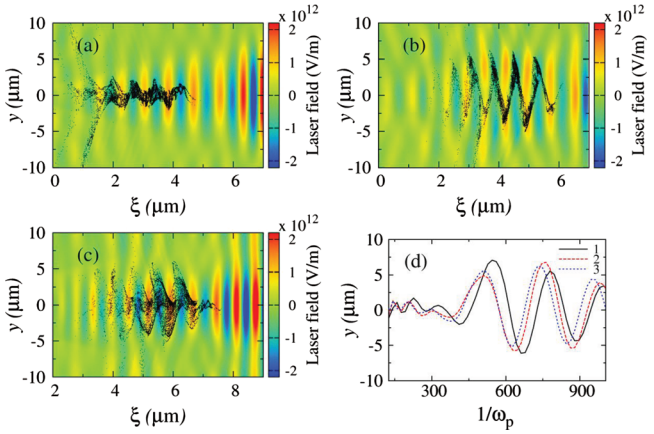

FIG. 3. (Color online) Distribution of electrons (black dots) and the laser field (background color figure) in the first ion cavity at (a) $t=2.44$ ps, (b) 4.16 ps, and (c) 5.74 ps. (d) Electron trajectories for three test particles, where the particles of label 1, 2, and 3 are located in the same phase of the laser field with a periodic distance of λ_0. In this simulation, the rising part and the falling part of the laser beam are 17.5 and 30 fs, respectively. Other parameters are the same as in Fig. 2.

lowered because the sharp rising duration of 7 fs is too short to generate wakefields effectively.

A. Electron motion in the ion cavity

Now, we describe the motion of the accelerated electrons inside the ion cavity in detail for the asymmetric (47.5 fs) laser pulse with a long falling time (30 fs, $9\,\mu \gtrsim$ m $\lambda_p/2$ in length). Figures 3(a)–3(c) show the accelerated electrons superimposed on the laser field. The electric field at the tail of the laser pulse is $E_0 \approx 2\times10^{12}$ V/m, which is one order of magnitude higher than the transverse focusing wakefield $E_t = 9.06\times10^{-15}\, n_e(\mathrm{cm}^{-3})\, r_\beta(\mu\mathrm{m}) = 27\times10^{11}$ V/m, where $n_e = 5\times10^{18}\,\mathrm{cm}^{-3}$, $r_\beta = 6\,\mu$m, for example. Thus, in this case, the force due to laser field dominates the interaction in the ion cavity.

In the rest frame of the electron beam, the electrons slip from the laser field because their velocity and the phase velocity of the laser field are different. In Fig. 3(d), we show the trajectories of three test electrons (labeled 1, 2, and 3) in the bunch, in which they are located at the same laser phase but longitudinally separated by one laser wavelength. Individual electron trajectories show transverse oscillations due to the phase-slip with the laser field. One can find that the wavelength of electron oscillation decreases unlike the wavelength of the betatron oscillation due to the focusing field of the wake wave, $\lambda_\beta = \sqrt{2\gamma}\,\lambda_p$, which means that the electron beam strongly interacts with the laser field. The electrons are accelerated in the direction of the laser polarization, resulting in increase of the amplitude of the transverse oscillations. The initial amplitude of the oscillations was approximately $1\,\mu$m in Fig. 3(a) at $t=2.44$ ps, after interaction with the laser fields, and the amplitude increased to the ion cavity size. Due to the combination of longitudinal and transverse forces, the electrons of the bunch are redistributed as a sinusoidal structure with a wavelength approximately similar to the wavelength of the laser field, as shown in Fig. 3(b). After the electrons reach a maximum amplitude (limited by the cavity size) of transverse oscillation, the sinusoidal structure deforms, as seen in Fig. 3(c).

B. Theoretical model

A simple harmonic oscillator model was proposed in Ref. 17 in order to describe the motion of accelerated electrons in the ion cavity. Here, we use this model for our studies and consider only the transverse motion. According to the model, the equation of motion is

$$\frac{d}{dt}[\gamma m \dot{y}] = -e\left(\frac{m\omega_p^2}{2e}y + E_y + \dot{x}B_z\right), \tag{1}$$

where $\omega_p^2 = 4\pi n_e e^2/m$, E_y and B_z are electric and magnetic fields of the laser pulse. It should be pointed out here that the theoretical model has a limitation as a gamma-factor of the bubble is not taken into account. The term $E_y + \dot{x}B_z$ in the right side of Eq. (1) is approximated by $E_y + \dot{x}B_z = 2E_y$ because of $dx/dt \simeq c$. We can assume the approximated solution as $x = v_e(t - t_0) + x_0$, where x_0 is the initial value of electron orbit at $t=t_0$, and v_e is the approximated electron velocity along x-direction, which is practically the speed of light c. The spatial and time variation of laser wave is expressed as $kx - \omega t = k(v_e(t-t_0) + x_0 - v_p t)$, where $v_p = \omega/k$ is the phase velocity of the laser wave. But due to the initial condition of $x=x_0$ at $t=t_0$, the term $x_0 - v_p t_0$ is almost zero. Therefore, the spatial and time variation of the laser wave is eventually expressed as $kx - \omega t = k(v_e - v_p)\tau$, where $\tau = t - t_0$ is the advancement of time after the electron beam enters the bubble at $x=x_0$. The polarized electric field E_y is expressed as $E_y(x,t) = E_0 \sin(kx - \omega t) = E_0 \sin[k(v_e - v_p)\tau]$. We define the phase-slip frequency by $\omega_\phi = k(v_e - v_p)$. Then, the polarized E-field is given by $E_y(x,t) = E_0 \sin(\omega_\phi \tau)$. After a straight forward calculation, Eq. (1) can be expressed as

$$\frac{d^2y}{dt^2} + 2\alpha\frac{dy}{dt} + \omega_\beta^2 y = -\frac{2a_0 c\,\omega}{\gamma}\sin(\omega_\phi\tau), \tag{2}$$

where the damping rate α is defined by $\alpha = (1/2\gamma)(d\gamma/dt)$ and the betatron frequency-squared due to the ion focusing is defined by $\omega_\beta^2 = \omega_p^2/2\gamma$. Here, it should be noted that the frequency ω is the laser frequency, which is much higher than the phase-slip frequency ω_ϕ or the betatron frequency ω_β. Due to the time variation of the relativistic energy factor γ of the electron beam, Eq. (2) is impossible to solve analytically. In this context, we assume that the relativistic energy factor is averaged over time to be $\gamma_b = <\gamma>$ during the whole dynamic process. It is obvious that Eq. (2) is a forced damping oscillation. Therefore, the simplified solution can be written as

$$y \simeq y_m \sin(\omega_\phi \tau), \tag{3}$$

where the maximum amplitude y_m is given by $y_m \simeq a_0\,\omega\, c/\gamma_b(\omega_\phi^2 - \omega_\beta^2)$. It should be noted that the betatron frequency ω_β by the focusing field of ions, which is decreased by the increased relativistic factor γ as the electrons are accelerated, is coupled with the phase-slip frequency ω_ϕ. From the PIC simulations, the averaged longitudinal velocity of electrons is

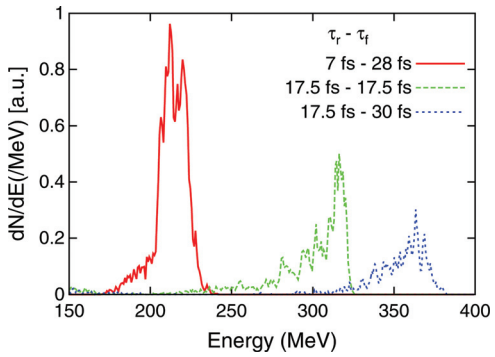

FIG. 4. (Color online) Energy spectra of the electron beams for different pulse shapes, consisting of various falling and rising durations.

$<v_x> \simeq 0.9984$ c, which is lowered due to large transverse motion of electrons. The electron density inside the bubble is $1 \times 10^{18}\,\mathrm{cm}^{-3}$, then the phase velocity of the laser is 1.00029c. Hence, we can assume that the phase velocity of the laser is almost equal to the speed of light near the ion cavity center, where the wavelength of the phase-slip oscillation is approximately 500 μm, as seen in Fig. 3(d). This is close to the wavelength of the betatron oscillation $\lambda_\beta \simeq 470\,\mu$m due to the focusing field of ions with the parameters $\gamma = 500$ and $\lambda_p = 15\,\mu$m. Then, two frequencies can be coupled to significantly increase the amplitude y_m of the transverse oscillation. After electrons reach the maximum amplitude of the transverse motion, this amplitude slightly decreases due to the increased gamma-factor of the electron beam which is accelerated to the center of the bubble. This amplitude is approximately five times larger than that of the case of the symmetric pulse shape in Fig. 2(c). Therefore, the wiggler strength parameter has increased from $a_\beta \simeq 6$ to $a_\beta \simeq 37$, corresponding to increase of the oscillation amplitude from $r_\beta \simeq 1\,\mu$m to $r_\beta \simeq 6\,\mu$m, based on an electron beam energy of $\gamma = 500$. The electron energy was also enhanced in case of asymmetric laser pulses when the rising duration of the pulse is the same as shown in Fig. 4. This could be due to the fact that electrons spend longer time in the acceleration phase of the ion cavity compared with the symmetric pulse case. The combined effect of the enhanced energy and the increased amplitude of the transverse oscillation can produce higher photon energies, resulting in x-ray radiation extending up to several tens of kiloelectronvolts.

IV. CONCLUSIONS

In conclusion, a temporally asymmetric laser pulse can be used for laser wakefield acceleration with self-injection and the tail part of the laser beam can interact strongly with the electron beam. This can lead to a large transverse electron oscillation due to the resonance, which can provide a good method for generation of ultrashort (~fs) coherent radiations covering tens of kiloelectronvolts in photon energy. The proposed scheme can be realized in a fairly simple experimental setup as temporally asymmetric laser pulses are easily produced by detuning the compressor gratings in a CPA (chirped-pulse amplification) laser system.[21]

ACKNOWLEDGMENTS

This research was financially supported by the Challenge Research Project of NRF (National Research Foundation) and SRC program (20100029421) of NRF of Korea.The authors would like to thank H.J Lee, S.W Hwang, and V. V. Kulagin for fruitful discussions.

[1]T. Tajima and J. M. Dawson, Phys. Rev. Lett. **43**, 267 (1979).
[2]S. P. D. Mangles, Z. N. C. D. Murphy, J. L. C. A. G. R. Thomas, A. E. Dangor, E. J. Divall, P. S. Foster, J. G. Gallacher, C. J. Hooker, D. A. Jaroszynski, A. J. Langley, W. B. Mori, P. A. Norreys, F. S. Tsung, R. Viskup, B. R. Walton, and K. Krushelnick, Nature (London) **431**, 535 (2004).
[3]C. G. R. Geddes, C. Toth, J. van Tilborg, E. Esarey, C. B. Schroeder, D. Bruhwiler, C. Nieter, J. Cary, and W. P. Leemans, Nature (London) **431**, 538 (2004).
[4]J. Faure, Y. Glinec, A. Pukhov, S. Kiselev, S. Gordienko, E. Lefebvre, J. P. Rousseau, F. Burgy, and V. Malka, Nature (London) **431**, 541 (2004).
[5]W. P. Leemans, B. Nagler, A. J. Gonsalves, C. Toth, K. Nakamura, C. G. R. Geddes, E. Esarey, C. B. Schroeder, and S. M. Hooker, Nat. Phys. **2**, 696 (2006).
[6]N. A. M. Hafz, T. M. Jeong, I. W. Choi, S. K. Lee, K. H. Pae, V. V. Kulagin, J. H. Sung, T. J. Yu, K.-H. Hong, T. Hosokai, J. R. Cary, D.-K. Ko, and J. Lee, Nat. Photon. **2**, 571 (2008).
[7]S. Kalmykov, S. A. Yi, V. Khudik, and G. Shvets, Phys. Rev. Lett. **103**, 135004 (2009).
[8]N. A. M. Hafz, S. K. Lee, T. M. Jeong, and J. Lee, Nucl. Instr. and Meth. A (unpublished).
[9]S. Kneip, C. McGuffey, J. L. Martins, S. F. Martins, C. Bellei, V. Chvykov, F. Dollar, R. Fonseca, C. Huntington, G. Kalintchenko, A. Maksimchuk, S. P. D. Mangles, T. Matsuoka, S. R. Nagel, C. A. J. Palmer, J. Schreiber, K. T. Phuoc, A. G. R. Thomas, V. Yanovsky, L. O. Silva, K. Krushelnick, and Z. Najmudin, Nat. Phys. **6**, 980 (2010).
[10]E. Esarey, B. A. Shadwick, P. Catravas, and W. P. Leemans, Phys. Rev. E **65**, 056505 (2002).
[11]A. Rousse, K. T. Phuoc, R. Shah, A. Pukhov, E. Lefebvre, V. Malka, S. Kiselev, F. Burgy, J.-P. Rousseau, D. Umstadter, and D. Hulin, Phys. Rev. Lett. **93**, 135005 (2004).
[12]B.-S. Xie, A. Aimidula, J.-S. Niu, J. Liu, and M. Yu, Laser Part. Beams **27**, 27 (2009).
[13]W. P. Leemans, P. Catravas, E. Esarey, C. G. R. Geddes, C. Toth, R. Trines, C. B. Schroeder, B. A. Shadwick, J. van Tilborg, and J. Faure, Phys. Rev. Lett. **89**, 174802 (2002).
[14]K. T. Phuoc, S. Corde, R. Shah, F. Albert, R. Fitour, J.-P. Rousseau, F. Burgy, B. Mercier, and A. Rousse, Phys. Rev. Lett. **97**, 225002 (2006).
[15]S. P. D. Mangles, A. G. R. Thomas, M. C. Kaluza, O. Lundh, F. Lindau, A. Persson, F. S. Tsung, Z. Najmudin, W. B. Mori, C.-G. Wahlström, and K. Krushelnick, Phys. Rev. Lett. **96**, 215001 (2006).
[16]A. G. R. Thomas and K. Krushelnick, Phys. Plasmas **16**, 103103 (2009).
[17]K. Németh, B. Shen, Y. Li, H. Shang, R. Crowell, K. C. Harkay, and J. R. Cary, Phys. Rev. Lett. **100**, 095002 (2008).
[18]J. Faure, C. Rechatin, A. Norlin, A. Lifschitz, Y. Glinec, and V. Malka, Nature (London) **444**, 737 (2006).
[19]A. V. Brantov, T. Z. Esirkepov, M. Kando, H. Kotaki, V. Y. Bychenkov, and S. V. Bulanov, Phys. Plasmas **15**, 073111 (2008).
[20]J. Faure, C. Rechatin, O. Lundh, L. Ammoura, and V. Malka, Phys. Plasmas **17**, 083107 (2010).
[21]N. A. M. Hafz, T. J. Yu, S. K. Lee, T. M. Jeong, J. H. Sung, and J. Lee, Appl. Phys. Express **3**, 076401 (2010).